Hyperfine Interactions and the Magnetic Fields Due to Core Polarization in Fe^{57}†

W. J. CHILDS AND L. S. GOODMAN
Argonne National Laboratory, Argonne, Illinois
(Received 9 August 1965; revised manuscript received 26 January 1966)

Magnetic-dipole hyperfine-interaction constants have been measured for the $^5D_{4,3,2,1}$ states of the ground term of Fe^{57} in an atomic-beam magnetic-resonance experiment. The values are $a_J = 38.0795(10)$, 26.351(2), 18.762(2), and 14.077(5) Mc/sec for $J = 4$, 3, 2, and 1, respectively. The deviations of the ratios of these a factors from theoretical predictions are ascribed to core polarization, and the implications of this assumption are discussed.

I. INTRODUCTION

THEORETICAL calculations of the magnetic-field intensity at the nucleus of an iron atom rely upon the concept of spin-polarization of the atomic electron core. Measurements of the hyperfine-interaction constant a for the $^5D_{4,3,2,1}$ states of the ground term of Fe^{57} atoms should yield information which would allow one to infer the amount of such core polarization in a system in which the atomic wave functions are relatively well known.

The work presented in this paper was initiated in order to acquire the data necessary to check theoretical estimates of the contribution of core polarization to the magnetic field at the nucleus.

II. EXPERIMENTAL DETAILS

A. Data Handling

The atomc-beam magnetic-resonance apparatus used for the present investigation has been described previously.[1] The machine was operated with the usual flop-in arrangement of the two 2-pole inhomogeneous magnetic fields.[2]

The detection system used to measure the beam intensity has been described previously.[1] Because the Fe^{57} is such a small fraction of the total iron in the atomic beam, the slit of the mass spectrometer was adjusted to discriminate strongly against the adjacent mass-56 atoms. This adjustment lowered the background counting rate considerably. The accelerating voltage of the mass spectrometer could be changed temporarily in order to focus Fe^{56} atoms onto its detector slit whenever it was desired to use a resonance of this component of the beam to set the homogeneous magnetic field.

The digital lock-in detector system, which has been described previously[1] was used in most of the experiment to enhance the signal-to-noise ratio of the resonance signals in Fe^{57}.

In this system the radio-frequency power applied to induce a transition is square-wave-modulated (100%). When the ratio frequency is on, a bi-directional scaler is gated to accumulate scaled counts from the electron-multiplier detector in the mass spectrometer. When the rf power is off, the counter is gated to subtract the scaled counts from the total accumulation.

After a time t the signal-to-noise ratio is $\eta = (s^2t/b)^{1/2}$, where b is the background counting rate and the signal rate s is the difference in counting rate induced by the application of radiofrequency power. In principle, any desired signal-to-noise ratio may be achieved by allowing t to become large enough. If, however, one is working with extremely small signal-to-background ratios, the time to achieve adequate signal-to-noise may become quite large and fluctuations other than statistical ones may make it impossible to make reliable comparisons of the counting rates for the different frequencies used in the scan of a resonance. Such fluctuations may be caused by changes in oven conditions with consequent change in beam intensity, drifts in mass spectrometer conditions with subsequent change in detection efficiency, or changes in the vacuum pressure with attendant changes of scattering both of beam atoms and of ions.

In order to work more reliably with small signal-to-background ratios, a new data-handling system was added to the existing equipment. The scaled counts from the electron multiplier are fed to the input of a multichannel scaler (MCS). The MCS address is advanced through a given number of channels by a crystal-controlled clock and the radiofrequency is swept stepwise in coordination with this channel-number advance. This process is repeated until an adequate signal-to-noise ratio is achieved.

Because the background counting rate is practically

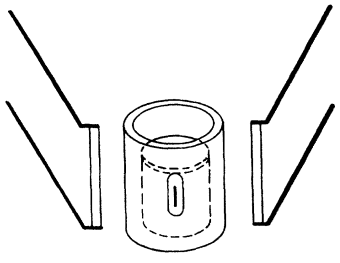

FIG. 1. Diagram of oven system. A tantalum shroud with a window contains the ZrO crucible. The tungsten emission filaments (which are spot welded to tantalum supports) are shown as a pair of vertical lines on each side of the oven.

† Work performed under the auspices of the U. S. Atomic Energy Commission.

[1] W. J. Childs, L. S. Goodman, and D. von Ehrenstein, Phys. Rev. **132**, 2128 (1963).

[2] N. F. Ramsey, *Molecular Beams* (Oxford University Press, New York, 1956).

the same for all channels in any one pass, it is not necessary to subtract the accumulated counts of the background. When the same signal-to-noise ratio has been reached at the peak of a resonance as with the digital lock-in technique, the noise is the same in all channels and a plot of the resonance looks just the same as it did with the old method except that it is added to a large but (within the noise limits) identical background.

Since it is not necessary to subtract background, the average signal rate is doubled. The expression for the signal-to-noise ratio η given above shows that the time to achieve a given η varies as the square of the signal rate. With the MCS system, the same signal-to-noise ratio can be obtained in a quarter of the time required in the digital lock-in system.

This advantage is sometimes partially sacrificed in practice by scanning a larger frequency range than is convenient with the single-channel scheme. On the other hand, the ability to sweep large regions reliably allows one to complete the experiment more rapidly. This latter advantage is more difficult to assess quantatively, but is also an important improvement over the old method of data handling.

The stepwise-swept radio frequency was measured by mixing with a crystal-locked local oscillator (Beckman-Berkeley Model 7570-71-72-73) and counting the difference frequency in the coordinated channels of the MCS. This method gives the average frequency applied during the time any one channel is in use.

Both the resonance information and the radio frequency as a function of channel number are read out of the MCS with a Monroe solid-state printer, Model MC-10-40.

B. Oven System

There is probably no completely satisfactory crucible material from which one can evaporate iron. A moderately satisfactory one consisted of a stabilized zirconium oxide crucible inside of a tantalum shroud (Fig. 1). The tantalum was heated by electron bombardment and the ZrO in turn was heated by conduction and radiation. The ZrO crucible frequently cracked upon being cooled so that many ovens were used during the course of the experiment.

It proved important to use pure iron with very low carbon content in order to minimize the tendency of the liquid iron to creep into and out of the slit. This liquid iron would alloy with the tantalum, block the beam, grow "whiskers" that would short to the electron-bombardment filaments, destroy the oven mount, etc.

TABLE I. The expected intensities of resonance signals in the $^5D_{4,3,2,1}$ states of the ground term of Fe^{57} relative to the unresolved resonance intensity in the ^5D term of even-even Fe^{56}.

State	Isotope	Relative intensity
^5D	Fe^{56}	1
$^5D_4$	Fe^{57}	0.0040
$^5D_3$		0.0029
$^5D_2$		0.0022
$^5D_1$		0.0018

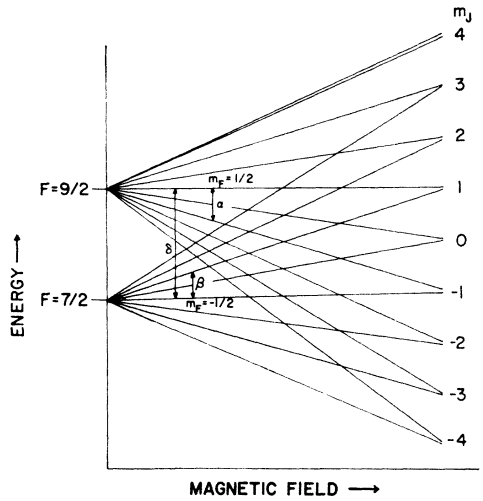

FIG. 2. Hyperfine-structure diagram for the $^5D_4$ state of Fe^{57}. The letters α and β indicate 2-quantum $\Delta F=0$ transitions. The letter δ indicates the $\Delta F=\pm 1$ transition whose frequency, when corrected to zero magnetic field, is equal to $(I+J)a_J$.

III. THE EXPERIMENT

The ground term of the free iron atom is ^5D which arises from the configuration $3d^64s^2$. For this term, the states that have a magnetic hyperfine interaction have electron angular momenta $J=4$, 3, 2, 1; all these states occur in the beam of iron atoms. Their occupation probabilities are the statistically weighted Boltzmann factors calculated for the oven temperature of 1600°C and the specific energy of excitation.

The intensity of the isotope of interest, Fe^{57}, is further reduced because it is only 2% abundant in the natural iron used in the experiment. Table I gives the expected relative intensities of the resonance signals. The Hamiltonian $\mathcal{H}$ for these neutral ground-term Fe^{57} atoms in an external magnetic field H is[2]

$$\mathcal{H}=a_J\mathbf{I}\cdot\mathbf{J}+g_J\mu_0(J_z+\gamma I_z)H, \qquad (1)$$

where a_J is the magnetic-dipole hyperfine-interaction constant for a particular state J, g_J is the electronic g factor, and γ is the ratio of the nuclear g factor to the electronic g factor.

The nuclear spin[3] $I=\frac{1}{2}$ and gyromagnetic ratio[4] $g_I=-\mu_I/I=-0.1806$ are well known. The g factor $g_J=1.50020(3)$ of the $^5D_4$ ground state has been measured by Kamlah[5] in Fe^{56}. Although g_J in the ^5D multi-

[3] N. S. Garifyanov, M. M. Zaripov, and B. M. Kozyrev, Dokl. Akad. Nauk SSSR **113**, 1243 (1957) [English transl: Soviet Phys.—Doklady **2**, 195 (1957)].

[4] G. W. Ludwig and H. H. Woodbury, Phys. Rev. **117**, 1286 (1960).

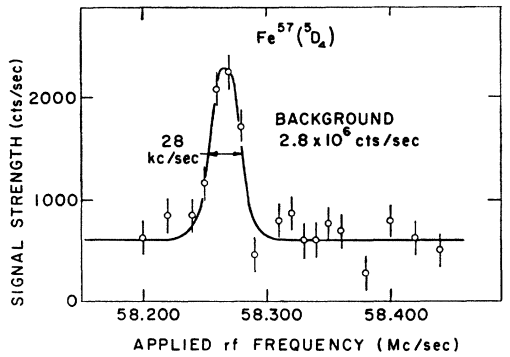

FIG. 3. Experimental resonance curve for the $\frac{7}{2},\frac{3}{2} \leftrightarrow \frac{7}{2},-\frac{1}{2}$ transition at 25G.

plet does have a slight J dependence,[6] it is so small that the above value could be assumed correct for the whole experiment without any sacrifice in the precision of the determined a factors.

The hyperfine-structure diagram of the $^5D_4$ state is shown in Fig. 2. The analogous diagrams for the $^5D_{3,2,1}$ states are entirely similar. The $\Delta F=0$, flop-in transitions α and β (indicated by arrows) are double-quantum transitions for which $\Delta m_F=2$.

To find the a factor for a given atomic state ^5D_J, we first looked for resonances corresponding to $\Delta F=0$, $\Delta m_F=\pm 2$ transitions at small magnetic fields. These resonances were followed up to higher magnetic fields and the a factor in Eq. (1) was adjusted to fit the data. An explicit expression for the resonant frequency as a function of a at magnetic field H has been given by Childs and Goodman.[7] This value of a could then be used to make predictions of resonances at higher magnetic fields. When the value of a_J was known precisely enough, a search for the $\Delta F=\pm 1$ transition δ was instituted. The observed $\Delta F=0$ and $\Delta F=\pm 1$ resonances along with the magnetic fields at which they were measured are listed in Table II. The frequency of the $\Delta F=\pm 1$ transition, corrected to zero magnetic field, is the hyperfine separation $\Delta\nu=(I+J)a_J$ from which a_J was evaluated. These values of the a_J are given in column 2 of Table III.

Figure 3 is a typical example of an observed resonance in Fe^{57}. The achievement of satisfactory signal-to-noise in spite of a quite small signal-to-background ratio is apparent.

IV. CORE POLARIZATION

To the extent that the iron atom is described by the Russell-Saunders coupling scheme, one can predict[8] the ratios for the a factors $a_J=r_J a_l$. The proportionality constant is $r_J=4/7$, $3/7$, $9/28$, $\frac{1}{4}$ for $J=4$, 3, 2, 1, respectively.

An attempt to describe the data in column 2 of Table III with a single parameter a_l results in the relatively poor fit given in column 3 of this table. The description of the data can be improved by assuming that part of the magnetic field at the nucleus is caused by spin polarization of the atomic electron core.[9]

To compute the core-polarization contribution of a given inner s-electron pair to the magnetic field at the nucleus one calculates $\psi(0)^2$ for the electron which has its spin parallel to the spin of the polarizing valence electron, and subtracts from this the calculated value of $\psi(0)^2$ for the other electron with antiparallel spin. This difference gives the induced spin density at the nucleus directly and thereby implies the magnetic field

TABLE II. The observed resonance frequencies of the experiment. The calculations which were used to obtain the entries in the column $\nu_{\rm obs}-\nu_{\rm calc}$ used the a values listed in Table III and $g_J=1.50020$. The $\Delta F=0$ resonances in the $^5D_1$ atomic state were observed as flop-out transitions.

Magnetic field (G)	Atomic state	Transition $F,m_F \leftrightarrow F',m_{F'}$	Resonance frequency (Mc/sec)	$\nu_{\rm obs}-\nu_{\rm cal}$ (kc/sec)
1	$^5D_4$	$\frac{7}{2},\frac{3}{2} \leftrightarrow \frac{7}{2},-\frac{1}{2}$	2.330(7)	−4(7)
3		$\frac{9}{2},\frac{1}{2} \leftrightarrow \frac{9}{2},-\frac{3}{2}$	5.600(7)	−2(7)
3		$\frac{7}{2},\frac{3}{2} \leftrightarrow \frac{7}{2},-\frac{1}{2}$	7.000(7)	−1(7)
15		$\frac{7}{2},\frac{3}{2} \leftrightarrow \frac{7}{2},-\frac{1}{2}$	35.011(5)	−1(5)
25		$\frac{7}{2},\frac{3}{2} \leftrightarrow \frac{7}{2},-\frac{1}{2}$	58.269(4)	2(4)
25.533		$\frac{9}{2},\frac{1}{2} \leftrightarrow \frac{9}{2},-\frac{3}{2}$	48.092(5)	−2(5)
30		$\frac{7}{2},\frac{3}{2} \leftrightarrow \frac{7}{2},-\frac{1}{2}$	69.838(10)	3(10)
50		$\frac{9}{2},\frac{1}{2} \leftrightarrow \frac{9}{2},-\frac{3}{2}$	95.454(6)	−8(6)
50		$\frac{7}{2},\frac{3}{2} \leftrightarrow \frac{7}{2},-\frac{1}{2}$	115.529(6)	−5(6)
1		$\frac{9}{2},\frac{1}{2} \leftrightarrow \frac{7}{2},-\frac{1}{2}$	173.470(6)	···
3	$^5D_3$	$\frac{5}{2},\frac{3}{2} \leftrightarrow \frac{5}{2},-\frac{1}{2}$	7.199(10)	−7(10)
5		$\frac{5}{2},\frac{3}{2} \leftrightarrow \frac{5}{2},-\frac{1}{2}$	12.015(10)	0(10)
10		$\frac{7}{2},\frac{1}{2} \leftrightarrow \frac{7}{2},-\frac{3}{2}$	18.150(7)	−5(7)
10		$\frac{5}{2},\frac{3}{2} \leftrightarrow \frac{5}{2},-\frac{1}{2}$	24.025(5)	0(5)
20		$\frac{7}{2},\frac{1}{2} \leftrightarrow \frac{7}{2},-\frac{3}{2}$	36.776(13)	−7(13)
20		$\frac{5}{2},\frac{3}{2} \leftrightarrow \frac{5}{2},-\frac{1}{2}$	47.815(13)	−5(13)
40		$\frac{7}{2},\frac{1}{2} \leftrightarrow \frac{7}{2},-\frac{3}{2}$	75.617(15)	−8(15)
40		$\frac{5}{2},\frac{3}{2} \leftrightarrow \frac{5}{2},-\frac{1}{2}$	93.713(5)	4(5)
1		$\frac{7}{2},\frac{1}{2} \leftrightarrow \frac{5}{2},-\frac{1}{2}$	94.349(7)	···
5	$^5D_2$	$\frac{3}{2},\frac{3}{2} \leftrightarrow \frac{3}{2},-\frac{1}{2}$	12.653(7)	2(7)
10		$\frac{5}{2},\frac{1}{2} \leftrightarrow \frac{5}{2},-\frac{3}{2}$	17.400(8)	9(8)
10		$\frac{3}{2},\frac{3}{2} \leftrightarrow \frac{3}{2},-\frac{1}{2}$	25.242(7)	20(7)
20		$\frac{3}{2},\frac{3}{2} \leftrightarrow \frac{3}{2},-\frac{1}{2}$	49.243(6)	14(6)
1		$\frac{5}{2},\frac{1}{2} \leftrightarrow \frac{3}{2},-\frac{1}{2}$	49.044(6)	···
20		$\frac{5}{2},\frac{1}{2} \leftrightarrow \frac{3}{2},-\frac{1}{2}$	104.642(10)	1(10)
2	$^5D_1$	$\frac{3}{2},-\frac{1}{2} \leftrightarrow \frac{3}{2},\frac{1}{2}$	2.822(10)	−2(10)
2		$\frac{3}{2},-\frac{1}{2} \leftrightarrow \frac{3}{2},-\frac{3}{2}$	3.972(10)	−1(10)
5		$\frac{3}{2},-\frac{1}{2} \leftrightarrow \frac{3}{2},\frac{1}{2}$	7.340(10)	3(10)
8		$\frac{3}{2},-\frac{1}{2} \leftrightarrow \frac{3}{2},\frac{1}{2}$	12.355(10)	4(10)
10		$\frac{3}{2},-\frac{1}{2} \leftrightarrow \frac{3}{2},\frac{1}{2}$	15.965(7)	3(7)
1		$\frac{3}{2},\frac{1}{2} \leftrightarrow \frac{1}{2},-\frac{1}{2}$	23.305(7)	···
10		$\frac{3}{2},\frac{1}{2} \leftrightarrow \frac{1}{2},-\frac{1}{2}$	50.356(8)	7(8)

[5] A. Kamlah, thesis, Erstes Physikalisches Institut, Universitat Heidelberg, 1962 (unpublished).

[6] W. J. Childs and L. S. Goodman, Phys. Rev. **140**, A447 (1965).

[7] W. J. Childs, and L. S. Goodman, Phys. Rev. **131**, 247 (1963).

[8] R. E. Trees, Phys. Rev. **92**, 308 (1953).

[9] R. Sternheimer, Phys. Rev. **86**, 316 (1952); A. J. Freeman and R. E. Watson, *ibid.* **131**, 2566 (1963); J. Bauche and B. R. Judd, Proc. Phys. Soc. (London) **83**, 145 (1964).

TABLE III. The measured a factors. Columns 3 and 4 are the residuals from a least-squares fit of the experimental data to theoretical predictions without and with core polarization, respectively.

State	a_J (Mc/sec)	$\Delta=a_{obs}-a_{calc}$ (Mc/sec) For $c=0$	For $c\neq 0$
$^5D_4$	+38.0795(10)	+2.0	+0.40
$^5D_3$	+26.351(2)	+0.6	−0.64
$^5D_2$	+18.762(2)	−1.5	−0.21
$^5D_1$	+14.077(5)	−1.7	+0.45
$\Sigma(\Delta)^2$		9.6	0.81
a_l		+63.1	+74.8
C		0.0	−5.1

associated with it.[10] Although the details of the calculation are complicated, the salient point for our needs is simple and apparent from the above discussion. The induced spin density, and thus the magnetic field due to core polarization, are parallel (or antiparallel) to the spin of the polarizing valence electron. The total magnetic field due to core polarization will therefore be $\mathbf{H}_c=c'\mathbf{S}$, where $\mathbf{S}$ is the total spin in the Russell-Saunders model and c' is a scalar constant. As Bausche and Judd[9] have observed, the spin is $\mathbf{S}=(\mathbf{L}+2\mathbf{S})-(\mathbf{L}+\mathbf{S})=(g-1)\mathbf{J}$ and thus $\mathbf{H}_c=c'(g_J-1)\mathbf{J}$. From this we see that the contribution to the magnetic hyperfine interaction energy is $-\mathcal{H}_c\cdot\mathbf{I}=-c'(g_J-1)\mathbf{I}\cdot\mathbf{J}$. For the states under consideration, g_J has practically the same value for $J=4, 3, 2, 1$. Therefore $-\mathbf{H}_c\cdot\mathbf{I}=c\mathbf{I}\cdot\mathbf{J}$ where c is independent of J; i.e., the magnetic hyperfine interaction associated with core polarization contributes the same additive constant c to the a factor for all of the states of the $^5D_{4,3,2,1}$ multiplet so that one can write

$$a_J=r_J a_l+c. \tag{2}$$

The least-squares fits to the data for this assumption are given in column 4 of Table III.

The contribution of core polarization to the hfs constant a is $c=-5.1$ Mc/sec. The value of a_l deduced by this least-squares fit is $a_l=74.8$ Mc/sec. This value of a_l is in satisfactory agreement with the value $a_l=70.7$ Mc/sec which can be calculated from the fine-structure constant $\zeta_{3d}(\mathrm{Fe})=382$ cm^{-1}.[8]

Dr. Paul Bagus of the Solid State Science Division of Argonne National Laboratory was kind enough to perform an unrestricted Hartree-Fock (uhf) calculation for the free Fe^{57} atom; the details can be found in the following paper in this journal.[11] For comparison with our experimental values, the pertinent results are the computed values $c=-4.4$ Mc/sec and $\langle 1/r^3\rangle_{av}=4.55a_0^{-3}$. This value of $\langle 1/r^3\rangle_{av}$ leads to a calculated a value[8]

$$a_l=R\alpha^2 a_0^3\left(\frac{m_e}{M_p}\right)\langle 1/r^3\rangle_{av}\, g_I=78.4 \text{ Mc/sec}.$$

[10] W. J. Childs and L. S. Goodman, Phys. Rev. **141**, 15 (1966).

[11] C. C. J. Roothan and P. S. Bagus, in *Methods in Computational Physics*, edited by B. Alder, S. Fernbach, and M. Rothenberg (Academic Press Inc., New York, 1963), Vol. II, p. 47.

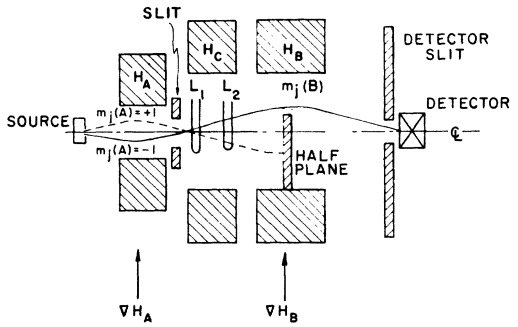

FIG. 4. Diagram of the atomic-beam machine modified for determining the algebraic sign of a.

V. THE MAGNETIC FIELD AT THE NUCLEUS

The magnetic field at the nucleus can be calculated from the relation[12]

$$-\mathbf{H}_{nuc}\cdot\boldsymbol{\mu}_n=ha_J\mathbf{I}\cdot\mathbf{J}=h(r_J a_l+c)\mathbf{I}\cdot\mathbf{J}. \tag{3}$$

The field-$hcIJ/\mu_n$ contributed by the core polarization is proportional to J, and (because of the relative signs of a_J and c) its direction is opposite to the field produced at the nucleus by the combined orbital and spin-dipole contributions of the d electrons.

For example, in the $J=4$ state Eq. (3) gives $H_{nuc}=-1.1\times10^6$ G. The contribution of core polarization is +150 kG. The magnetic field at the nucleus and the contribution of core polarization to this field for each J are given in Table IV.

VI. THE ALGEBRAIC SIGN OF THE a FACTOR

After correction for the effect of core polarization, the ratios r_J agree quite well with the theoretical predictions. It was therefore considered necessary to check the sign of the a factor for the $J=4$ state only.

The experimental method used was a slight modification of the "flop-out on flop-in" scheme of Jaccarino and King.[13] In this scheme, the characteristics of the atomic beam machine are changed by adding a half plane (Fig. 4) to block all atoms that undergo refocus-

TABLE IV. Total magnetic field at the nucleus and the magnetic field at the nucleus due to core polarization.

Atomic state	H_{nuc} (10^6G)	$H_{c.p.}$ (10^3G)
$^5D_4$	−1.1	+150
$^5D_3$	−0.57	+110
$^5D_2$	−0.27	+ 73
$^5D_1$	−0.10	+ 36

[12] H. Kopfermann, *Nuclear Moments* (Academic Press Inc., New York, 1958), p. 131.

[13] J. G. King and V. Jaccarino, Phys. Rev. **94**, 1610 (1954); W. J. Childs, L. S. Goodman, and L. J. Kieffer, *ibid.* **120**, 2138 (1960).

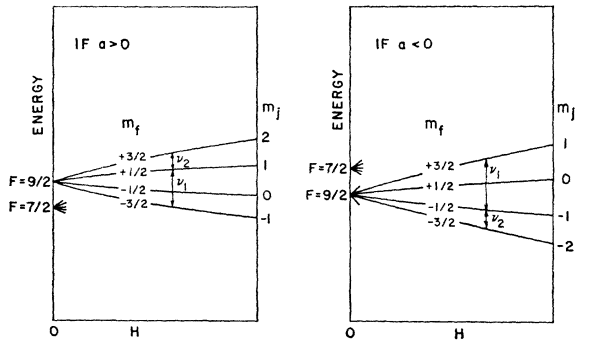

FIG. 5. Portions of the hfs diagrams of the $^5D_4$ state for the two possible cases: $a<0$ and $a>0$.

ing transitions such that they have $m_J<0$ in the B magnet. The dashed curve in the figure represents such a blocked trajectory.

Figure 5 shows the pertinent portion of the hfs diagrams for the two possible cases $a>0$ and $a<0$. The important feature to be noticed is that a difference in the sign of a corresponds to a reversal of the ordering of the zero-field hyperfine levels. This difference in ordering requires that the refocusing transitions observable in the modified machine, as described above, take place between different pairs of states for $a>0$ and $a<0$. The refocusable transitions used are $\frac{9}{2}$, $-\frac{3}{2}$, $\rightarrow \frac{9}{2}$, $\frac{1}{2}$ for $a>0$ and $\frac{9}{2}$, $-\frac{1}{2} \rightarrow \frac{9}{2}$, $\frac{3}{2}$ for $a<0$. If $a>0$, the state of the refocused atoms is characterized by the quantum number $m_F=\frac{1}{2}$ and a further transition in the C field at frequency ν_2 would cause them to go from $m_F=\frac{1}{2}$ to $m_F=\frac{3}{2}$. If $a<0$ the refocused atoms have $m_F=\frac{3}{2}$. Subsequent application of rf power at ν_2 (the transition frequency between states with $m_F=-\frac{1}{2}$ and $m_F=-\frac{3}{2}$) can have no effect on the refocused atoms. Applying radiofrequency power at the flop-in frequency ν_1 in loop L_1 increases the number of atoms that can reach the detector slit along the solid-line trajectory (Fig. 4). Application of rf power at the flop-out frequency ν_2 in loop L_2 will cause some of these refocused atoms to follow the dotted trajectory away from the detector slit if $a>0$ but will cause no change in the intensty of the refocused atoms if $a<0$.

If, on the other hand, rf power at frequency ν_2 is applied in loop L_1, the analysis is changed. For $a>0$, the transitions induced in loop L_1 are between $m_F=\frac{1}{2}$ and $m_F=\frac{3}{2}$. These have no effect on the initial state of the refocusable transition which can now be induced by the application of ν_1 in loop L_2. For $a<0$, however, transitions induced at frequency ν_2 in loop L_1 populate the $m_F=-\frac{1}{2}$ state with atoms that had $m_J(A)=-2$. These atoms can now undergo transitions at frequency ν_1 in loop L_2 but their history in the A magnet will prevent them from refocusing.

Since the value of a was known, ν_1 and ν_2 could be calculated with precision for a given magnetic field intensity. The C-field setting was chosen so that ν_1 and ν_2 were many line widths apart. At the magnetic field $H=100$ G used in the measurement, the "flop-in and flop-out"[13] frequencies were $\nu_1=195.903$ Mc/sec and $\nu_2=193.260$ Mc/sec.

It was more efficient, since no frequency search was necessary, to perform this portion of the experiment with the single-channel, digital, lock-in system. The rf power at the flop-in resonance frequency ν_1 was square-wave modulated and applied to the appropriate loop. The difference in counting rate between rf-on and rf-off was integrated for some time T until adequate signal-to-noise was attained. Radio frequency power at frequency ν_2 was then applied to the other loop and the differential counting rate was integrated for the same length of time T.

With ν_1 on loop L_1, applying ν_2 to loop L_2 decreased the integrated counts by about 60%. With the order reversed, i.e., with ν_1 applied to loop L_2, applying ν_2 to loop L_1 had no measurable effect on the counting rate. The algebraic sign of a is therefore positive.

VII. DISCUSSION

Assuming spin polarization of the atomic core leads to a good fit between the experimental determinations of the a factors of the ^5D ground multiplet of Fe^{57} and the theoretical hfs constants predicted on the basis of the Russell-Saunders model. The fit of the experimentally determined values of c and a_l to the predictions of Bagus's *ab initio* uhf calculation provides strong support for the assumption that the need for the parameter c to fit the empirical a factors is a manifestation of core polarization.

ACKNOWLEDGMENTS

The authors are indebted to Dr. Paul Bagus who performed the unrestricted Hartree-Fock calculations of $\langle 1/r^3 \rangle_{av}$. They would also like to thank Dr. Brian Wybourne for helpful discussions.